DEVELOPMENT OF HYDROGEN ISOTOPE-

RATIO MASS SPECTROMETRY FOR

ORGANOCHLORINE MOLECULES

By

WILLIAM RHEA ALLEY, JR.

Bachelor of Science

Dickinson State University

Dickinson, North Dakota

2000

Submitted to the Faculty of the Graduate
College of the Oklahoma State University
in partial fulfillment of the Degree of
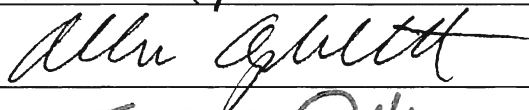MASTERS OF SCIENCE
August, 2002

DEVELOPMENT OF HYDROGEN ISOTOPE-

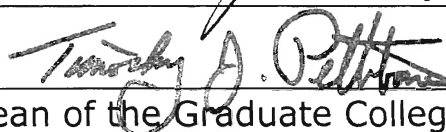# RATIO MASS SPECTROMETRY FOR

ORGANOCHLORINE MOLECULES

Thesis Approved:

_____
Thesis Adviser

_____

_____

_____
Dean of the Graduate College

ACKNOWLEDGEMENTS

TABLE OF CONTENTS

LIST OF TABLES

v

LIST OF FIGURES

NOMENCLATURE/SYMBOLS

B .... magnetic field strength
C .... degrees Celsius
CO .... carbon monoxide
CO_2 ....carbon dioxide
CuO .... copper (II) oxide
DH .... deuterium hydride
D/H .... deuterium-to-hydrogen ratio
F_C .... centripetal force
F_M .... magnetic force
GC .... gas chromatograph
H_2 .... hydrogen
HCl .... hydrogen chloride
He .... helium
i .... electric current
IRM .... isotope-ratio monitoring
IRMMS .... isotope-ratio monitoring mass spectrometry
KE .... kinetic energy
m .... mass
MS .... mass spectrometer/mass spectrometry
m/q .... mass-to-charge ratio
N_2 .... nitrogen
O_2 .... oxygen
q .... electric charge
r .... radius
RC .... reduction capacity
RE .... reduction efficiency
TE .... transmission efficiency
v .... velocity
UHP .... ultra high purity
‰ .... "per mil"

CHAPTER 1

INTRODUCTION

Hydrogen isotopes have a large relative mass difference and a wide range of isotope ratios are found in nature. Because of these properties, and recent advances in mass spectrometry instrumentation, hydrogen-isotope ratios recently have found several applications in different fields including the use as chemical markers [1, 2, 3], flavor authentification [4], and biolipid synthesis [5].

One field that has only recently started to take advantage of hydrogen-isotope ratios is the environmental sciences. In this field, hydrogen isotopes are used mainly as indicator for bioremediation of petroleum-based compounds [6, 7,8], many of those compounds (benzene, toluene ethyl benzene) are known to pose threats to human health. However, many other chemicals present in the environment posses threats to human health, including organochlorine molecules such as dioxins, furans, PCBs, and various chlorinated solvents. To minimize human health threats, their behavior in the environment, reactions they undergo, their transport paths and mechanisms, and their final fate, must be known.

At the present time, current instrumentation cannot make accurate hydrogen isotope-ratio measurements of organochlorine molecules online due to fractionation of hydrogen isotopes with

1

chlorine during pyrolysis, the accepted method of generating hydrogen on-line. Fractionation of isotopes leads to inaccurate data, therefore to acquire accurate data, hydrogen chloride, a major product of pyrolysis of organochlorine molecules, must be reduced. The aim of this project was to develop a method to reduce HCl on-line for hydrogen isotope-ratio monitoring mass spectrometry of organchlorine molecules.

DEVELOPMENT OF THE ISOTOPE-RATIO MONITORING MASS SPECTROMETER (IRMMS)

Using mass spectrometry to study isotope ratios began in 1940, when Nier built the first isotope-ratio monitoring mass spectrometer (IRMMS) [8]. Modern IRM mass spectrometers are still based on this design. The mass spectrometer Nier built consisted of an electron-impact ionization source using a tungsten filament, a curved flight tube with a permanent magnet for mass separation, and a single collector system using an "electrometer tube," the forefather of today's electron multiplier tube [8].

In a magnetic sector mass spectrometer, two forces, the centripetal force, F_C, and the magnetic-field force, F_M, must be equal for a detected ion to have the correct radius [9].

$$F_C = F_M \qquad\qquad \text{(Eq. 1)}$$

F_C is defined as $(mv^2)/r$ where m is the mass of the ion in kilograms, v is the velocity of the ion in meters per second, and r is the radius of the curved flight tube in meters. F_M is defined as qvB where q is the charge on the ion in Coulombs, v is the velocity of the ion in meters per second, and B is the magnetic field strength in Tesla [9].

Substituting these definitions into Equation 1 yields

$$(mv^2)/r = qvB \qquad \text{(Eq. 2)}$$

Equation 2 can be rearranged as:

$$mv = qBr \qquad \text{(Eq. 3)}$$

Kinetic energy, KE, is equal to $(1/2)mv^2$ and KE is also equal to qV_s for an ion that is accelerated through a potential difference [9].

$$KE = (1/2)mv^2 = qV_S \qquad \text{(Eq. 4)}$$

$$mv^2 = 2qV_S \qquad \text{(Eq. 5)}$$

Squaring both sides of Equation 3 and dividing by Equation 5 yields

$$m = (qB^2r^2)/(2V_S) \qquad \text{(Eq. 6)}$$

Equation 6 can be rearranged to give

$$(m/q) = (B^2r^2)/(2V_S) \qquad \text{(Eq. 7)}$$

From Equation 7, different mass-to-charge ratios, m/q, can be detected at a set radius given the proper B and V values [9].

The basic design of Nier's instrument was continually improved. In 1947, a dual-collector system was developed, allowing both

isotopes of interest to be collected simultaneously [10]. This instrument was further refined when McKinney *et al.* introduced a dual inlet system [11]. This advancement allowed for the rapid introduction of a standard working gas for comparison to the gas of interest. The ability to rapidly switch between reference and sample gases was necessary to minimize instrument drift [11].

OFF-LINE METHODS OF ANALYSIS

Using a dual-inlet instrument required off-line methods, methods of producing gas that are not incorporated into the instrumentation, for producing gases to be used for isotopic analysis. Several variations exist on a common theme for producing gas off-line from organic samples. The work presented here dealt only with hydrogen, therefore only off-line production of hydrogen will be discussed. Methods for off-line production of other gases for stable isotope analyses can be found in references 12 and 13.

For a generalized method for producing hydrogen off-line, a sample, containing approximately 10^{-6} moles of hydrogen [12, 13], is introduced to a quartz tube, sealed, evacuated, and combusted over CuO wire at 800 °C to 1000 °C. At these temperatures, equilibrium exists between CuO and O_2 [14], and the O_2 released by the CuO is used for combustion. The sample is continuously circulated through

calculated the same as R_{SMPL}. For hydrogen-isotope analyses, these ratios are deuterium-to-hydrogen.

Generally, changes in isotope ratios are very small, occurring in the fourth or fifth decimal points. Using an absolute ratio, these changes may be hard to locate. Using delta notation allows the analyst to eliminate the leading several digits that remain unchanged [14]. Subtle changes in the isotope ratio appear as more obvious changes in delta notation. Delta values are referred to as "per mil" and the symbol "‰" is used to denote per mil [14].

Delta values are reported against an isotopic standard because the relative isotope ratio is more accurate and easier to obtain than the absolute isotope ratio. Several standards are used depending on the isotopes being analyzed. For carbon isotopes, the standard is PeeDe Belemite, abbreviated as PDB. The large variation in the natural D/H isotope ratio results in the necessity of several standards to avoid errors data analysis. Standards used in hydrogen-isotope analysis include Standard Light Arctic Precipitation, or abbreviated as SLAP, Standard Mean Ocean Water, SMOW, Vienna Standard Mean Ocean Water, VSMOW, Greenland Standard Light Precipitation, GSLP. Air is used as the nitrogen-isotope standard, and Canyon Diablo Triolite for sulfur isotopes. SMOW and PBD are used for oxygen isotopes [19].

ON-LINE HYDROGEN IRMMS

Developing an on-line method to acquire accurate δD values for hydrogen proved to be a difficult task. Three problems existed for hydrogen IRMMS: 1) quantitatively producing hydrogen on-line, 2) removing $^4He^+$ from the DH signal, and 3) adopting an H_3^+ factor for an on-line method.

ONLINE PRODUCTION OF HYDROGEN

Burgoyne and Hayes achieved complete quantitative pyrolysis of organic molecules in 1998 using a graphitized-alumina tube and a silicon carbide electrical heating element known as a "Globar" [20]. The maximum signal occured at about 1440 °C and then decreased. The decrease in signal was attributed to the formation of cracks in the alumina tube at higher temperatures. With this method, the need for metal catalysts was eliminated and it has become the accepted method for on-line production of hydrogen.

REMOVING $^4He^+$ FROM DH

Helium, the carrier gas used in on-line methods, becomes ionized to $^4He^+$ in the ion source of the mass spectrometer [18, 21, 22]. After leaving the ion source, a helium ion may collide with a helium atom and lose kinetic energy, causing the ion to change its

original path and become scattered. A part of this scattered ^{4}He$^+$ will

have low enough energy arrive in the DH mass-3 Faraday cup [23].

The signal generated by lower-energy mass-4 helium ions is 10^4 to 10^5

times stronger than the signal generated by the deuterium-hydrogen

molecules, overwhelming any signal generated by DH [21].

Commercial isotope-ratio monitoring mass spectrometers are low-

resolution instruments unable to resolve DH from ^{4}He$^+$.

To eliminate noise generated by ^{4}He$^+$, an electrostatic retarding

lens was added before the mass-3 Faraday cup in the detector [24].

Only ions with kinetic energies greater than ~2250 eV are transmitted

through the lens. Background signals generated by helium are

reduced to less than 75 femtoamps, [5] approximately 2% to 2.5% of

a typical signal in this study. The helium background signal does not

increase with increasing flow rate [24].

THE H$_3^+$ FACTOR

H$_3^+$ is formed in the ion source of the mass spectrometer by the

reaction process [25, 26]:

$$H_2^+ + H_2 \rightarrow H_3^+ + H^{\cdot} \qquad \text{(Reaction 1)}$$

The concentration of H$_3^+$ is proportional to the square of the partial

pressure of the hydrogen in the ion source [25, 26]. During a

hydrogen-isotope analysis, the mass 3-to-mass 2 ratio, (D/H), is

calculated from the peak areas from the respective masses, or the ratio is calculated from the current generated by the respective masses. The total current detected for mass 3 is given as:

$$i_3 = i_{DH} + i_{H3}^+ \qquad \text{(Eq. 8)}$$

where i is the current measured [25]. From this equation, it can be seen that the presence of H_3^+ can effect the accuracy of the mass 3-to-mass 2 ratio. Substituting ion currents for partial pressures in Equation 8 shows

$$i_{H3}^+ = K(i_{H2})^2 \qquad \text{(Eq. 9)}$$

where K is an experimentally determined proportionality constant, commonly referred to as the "H_3^+ factor" [25]. To determine the mass 3-to-mass 2 ratio, the mass-3 ion current is divided by the mass-2 ion current [25] or

$$R = (i_{HD} + i_{H3}^+)/i_{H2} = i_{HD}/i_{H2} + Ki_{H2} \qquad \text{(Eq. 10)}$$

with R as the measured ion-ratio current [25].

To determine the value of K, i_{H2} is varied by simply increasing the pressure of the reference gas on a dual inlet mass spectrometer. Equation 10 is linear, and K is taken to be the slope of the regression line [25]. Important requirements for the H_3^+ factor are that it should be small, but, more importantly; it must be reproducible and constant.

ON-LINE HYDROGEN ANALYSIS OF ORGANOCHLORINE COMPOUNDS

While the on-line method developed for hydrogen-isotope analysis is effective for hydrocarbons, reported precisions of approximately ±5‰ [5], problems arise when this method is applied to organochlorine molecules. When organochlorine molecules are pyrolyzed, a wide range of products is formed. Hydrogen chloride is a major product that is detected for a number of molecules, such as CH_2Cl_2, CH_3Cl, and C_2HCl_3 [27-31].

Unpublished data from Burgoyne, Sessions, and Hayes suggests that hydrogen-isotope fractionation occurs during the pyrolysis of organochlorine molecules. To test isotope fractionation between H_2 and HCl, nine aliquots of methyl chloride gas were injected in helium (flow rate ~1 ml/min) through a pyrolysis reactor using an 8-port valve producing hydrogen gas and hydrogen chloride gas. The products entered a reduction oven containing chromium at 850 $^{\circ}$C to reduce HCl to H_2. Hydrogen gas then entered a MAT 252 mass spectrometer for isotopic analysis. In this manner, δD values were obtained for all of the hydrogen present in the methyl chloride. A second series of nine aliquots of methyl chloride were injected with the capillary between the pyrolysis furnance and the reduction oven immersed in a Dewar of liquid nitrogen. This trap froze HCl produced by pyrolysis and removed it from the gas stream. The HCl was not allowed to

enter the chromium reduction reactor and was not reduced to H_2. Delta-D values obtained for the second series of nine injections were for H_2 produced by pyrolysis only, leaving the chlorine-bound hydrogen unaccounted for in the δD values. If no fractionation occurred, the δD values would be the same for both series of injections. The δD for the first, fifth, and ninth injections was set to arbitrarily set to zero. The average δD for the first nine injections, where the hydrogen entering the mass spectrometer was the total hydrogen present (H_2 produced by pyrolysis and H_2 produced by reducing HCl) on the methyl chloride was 0.37 ± 1.95 (average and standard deviation). The average δD for the tenth through eighteenth injections, (H_2 produced by pyrolysis only) was -23.55 ± 2.69. Hydrogen generated by pyrolysis is depleted in deuterium, as shown by the more negative δD values for the tenth through 18th peaks, leaving the HCl generated enriched in deuterium.

For the accurate hydrogen isotopic analysis of organchlorine molecules, the hydrogen must be liberated from HCl, a major pyrolysis product of chlorine-containing organic compounds.

CHAPTER 2

EXPERIMENTAL

DEVELOPING THE CATALYST SYSTEM

The general process for quantitative production of hydrogen gas from organochlorine molecules is pyrolysis followed by reduction of the chlorine-bound hydrogen.

To determine the best catalyst for reducing an aliquot of HCl in a stream of helium with a flow rate of ~1 ml/min, several metals (listed in Table 1) were initially tested for two traits: 1) the transmission efficiency, the relative amount of hydrogen adsorbed by the metal, and 2) the reduction efficiency, the relative amount of HCl reduced by the metal.

Table 1. Metals and diameters tested for transmission and reduction efficiencies.

Metal	Diameter	Company
Aluminum	0.125 mm	Aldrich
Chromium	200 mm powder	Goodfellow
Magnesium	0.25 mm	Goodfellow
Manganese	-325 mesh powder	Aldrich
Molybdenum	0.25 mm	Aldrich
Nickel	0.25 mm	Aldrich
Palladium	0.10 mm	Aldrich
Platinum	0.10 mm	Aldrich
Silver	0.127 mm	Aldrich
Stainless Steel[a]	0.10 mm	Goodfellow
Vanadium	0.25 mm	Goodfellow
Zinc	0.25 mm	Goodfellow

a. alloy 302 containing 78% iron, 18% chromium, 8% nickel.

An ideal catalyst would have both high transmission and reduction efficiencies, in addition to having no memory effect, or causing isotope fractionation of the sample. It should also display fast adsorption/desorption properties to limit peak tailing.

TRANSMISSION EFFICIENCY

Transmission efficiency, TE, is defined as the average peak area at each temperature, divided by the average peak area from the blank tube. Transmission efficiency provides a measure of the hydrogen absorbed by a given metal. The maximum possible TE is 1, indicating the catalyst absorbed no hydrogen,

To determine the transmission efficiency, the each metal was inserted into the entire length of a grade 0.998 alumina tube with a length of 12 inches, an inner diameter of 1/32 inch, and an outer diameter of 1/16 inch (McDanel-Vesuvius, Beaver Falls, PA). The metal was heated for a minimum of five hours under a UHP helium atmosphere (Stillwater Steel, Stillwater, OK) in the reduction oven of a GC Combustion III interface (ThermoFinnigan, Bremen, Germany) at a temperature 100 $^\circ$C below the metal's melting point or 1000 $^\circ$C, whichever was the lower temperature. The temperature was monitored with a type S thermocouple (Omega Engineering, Stamford, CT). Using an 8-port valve, (Valco, Houston, TX) ten aliquots, each

containing $\sim 10^{-9}$ moles of hydrogen, of propane (Air Gas, Stillwater, OK) were injected, one every 200 seconds and pyrolyzed in a graphitized-alumina tube. The flow rate into the pyrolysis furnace was ~ 0.8 ml/min. Alumina tubes were graphitized by injecting ~ 10 µl of hexane via the injection port on the GC. Hydrogen gas was detected with a ThermoFinnigan Delta^{Plus} XL isotope-ratio monitoring mass spectrometer (ThermoFinnigan, Bremen, Germany) with a 75 µm inner diameter capillary 1.5 meters in length as the inlet capillary. Temperatures were varied from $\sim 25\ ^{\circ}$C to $\sim 100\ ^{\circ}$C below the melting point of the metal or until the transmission efficiency began to decline. The system was allowed to equilibrate for a minimum of two hours before further injections were done after changing temperatures. Runs with blank tubes were performed at $100\ ^{\circ}$C.

REDUCTION EFFICIENCY

Reduction efficiency, RE, is defined as the average peak area before using the liquid nitrogen trap divided by the average peak area after using the liquid nitrogen trap. The ratio of hydrogen peak areas before and after using the liquid nitrogen trap is a measure of the metal's ability to reduce HCl on-line.

The maximum reduction efficiency is 1.25. Pyrolysis of ethyl chloride follows the reaction:

$$C_2H_5Cl \rightarrow 2H_2 + HCl \qquad \text{(Reaction 2)}$$

If HCl is allowed to enter the reduction oven (the liquid nitrogen trap is not used), the maximum amount of hydrogen generated is given as:

$$2H_2 + HCl \rightarrow 2.5H_2 \qquad \text{(Reaction 3)}$$

If HCl is not allowed to enter the reduction oven (the liquid nitrogen trap is used), the reaction is the same as Reaction 2. If all HCl generated is reduced, the ratio of the area before using the liquid nitrogen trap to the area after using the liquid nitrogen trap will be 2.5/2 or 1.25.

Metals with favorable transmission efficiencies were tested for reduction efficiencies. Using a similar method as described above, five aliquots of ethyl chloride (Stillwater Steel, Stillwater, OK) were injected and pyrolyzed, with each aliquot containing $\sim 10^{-9}$ moles hydrogen. After allowing the fifth aliquot to completely elute, the capillary tube between the pyrolysis furnace and the reduction oven was immersed in a Dewar containing liquid nitrogen. Such a trap removes by freezing any HCl formed by pyroloysis from the helium stream and thus chlorine-bound hydrogen is not reduced. Data collected below 1150 °C were acquired using a NiChrome (Omega Engineering, Stamford, CT) resistive wire-heating element. Temperatures above 1150 °C were achieved using a 12-inch Globar, one-half inch in diameter, and with a 5-inch hot zone (MEG Systems,

Carrolton, TX), powered by a 22-amp variable transformer (Superior Electric, Bristol, CT) via a solid-state relay (Omega, Stamford, Connecticut).

To determine the volume of hydrogen present on the gases injected, a 125 ml gas-sampling bulb (Alltech Chromatography, Deerfield, IL) was filled with hydrogen tank gas. Assuming the pressure inside the bulb was the same was as the pressure read on the tank regulator and knowing the volume of gas injected into the GC, the moles of hydrogen were calculated using the ideal gas law. The temperature of the gas was assumed to be 298 K. Several volumes were injected over the range of 10 µl to 50 µl using a gas-tight syringe (SGE Chromatography, Houston, TX.) Plotting peak area versus moles of hydrogen injected gave a straight line. After finding the equation of that line, and substituting area for the hydrogen from the ethyl chloride for y and solving the equation for x gave the moles of hydrogen injected. The pressure on the ethyl chloride was then adjusted to inject $\sim 10^{-9}$ moles hydrogen injection.

EFFECTS OF LEAKS

A typical isotope-ratio monitoring mass spectrometry system has many connections, allowing for many sources of possible leaks. Detecting minor leaks can be a tedious, time-consuming procedure.

To determine the effect of oxygen on the ability of 302 stainless steel to reduce HCl, UHP oxygen (Stillwater Steel, Stillwater, OK) was introduced into the system between the reduction oven and pyrolysis furnace, at a point after the liquid nitrogen trap at a flow rate of 0.005 ml/min. (All future references to stainless steel are for alloy 302.) The effects of the simulated leak can be seen in the background scans before and after introducing oxygen to the system (see page 33). After allowing the oxygen to flow for one hour, the reduction efficiency experiment was again repeated. Oxygen was allowed to flow through the system during the time between temperature changes.

REDUCTION CAPACITY

Reduction capacity, RC, is defined as the maximum moles of HCl that can be reduced by stainless steel on-line before a significant decrease in reduction efficiency occurs. Ideally, the catalyst would be capable of reducing a large amount of HCl and would not require frequent changing.

To determine the reduction capacity of stainless steel, the reduction efficiency experiment was repeated with the catalyst at 1225 $^{\circ}$C, the optimum operating temperature, until the reduction efficiency began to decease. Each injection of ethyl chloride contained $\sim 10^{-9}$ moles of hydrogen.

ON-LINE ANALYSIS OF PCBs

The ultimate test for the system was to analyze samples of known δD. If the system failed to give accurate and reproducible results, or caused isotope fractionation, or had a memory effect, a new catalyst would need to be developed.

To test whether the system could reduce HCl and give accurate δD values, a series of PCBs of known δD were analyzed on-line using stainless steel at 1225 °C. The on-line values were compared against off-line values acquired by Dr. Arndt Schimmelmann at Indiana University, Bloomington. To determine the off-line δD, each sample was loaded into a 9-mm outer diameter quartz cuvette containing copper (II) oxide, copper and silver, and was then combusted [32].

To standardize the hydrogen tank gas, three 25-second injections of hydrogen tank gas were introduced into the mass spectrometer via the reference-gas inlet located in the combustion interface. A series of five hydrogen gas samples of known δD, also determined by Dr. Arndt Schimmelmann [1], were injected via the gas chromatograph. Plotting the δD value versus the measured D/H ratio gave a straight line. After finding the equation of the line, the D/H ratio of the hydrogen tank gas was substituted in for x. Solving the equation of y, the δD of each injection of the hydrogen tank gas was

20

calculated. The average δD for the three injections was used as the reference δD value.

After melting the PCBs in a hot-water bath, $\sim10^{-8}$ to 10^{-9} moles of each PCB was injected into an HP 6890 GC (Hewlett Packard, Wilmington, DE).   The injection port and oven temperatures were both set 280 $^\circ$C. Each PCB was injected one or two times per run using a 1-μL syringe (SGE Chromatography, Houston, TX). Two 25-second peaks of previously standardized reference hydrogen gas were injected prior to the injection of the PCBs using the reference-gas inlet. The stainless steel was changed after every four injections and heated for at least five hours at 1225 $^\circ$C. H_3^+ correction factors calculated after every two injections. The off-line δD values can be found in Table 2 for the PCBs analyzed.

Table 2. Off-line delta values for the PCBs used.

PCB	Off-line δD
4-chloro	-49.7, -55.9
3,4-dichloro	-77.1, -68.7
2,3',4-trichloro	-22.5, -27.6

Chapter 3

RESULTS AND DISCUSSION

TRANSMISSION AND REDUCTION EFFICIENCY

Figures 2 through 11 are transmission efficiency plots for the metals tested. Figures 12 through 17 are reduction efficiency plots for metals with a high transmission efficiency. Reduction efficiency plots are shown with the transmission efficiency for easy comparison of the two values.
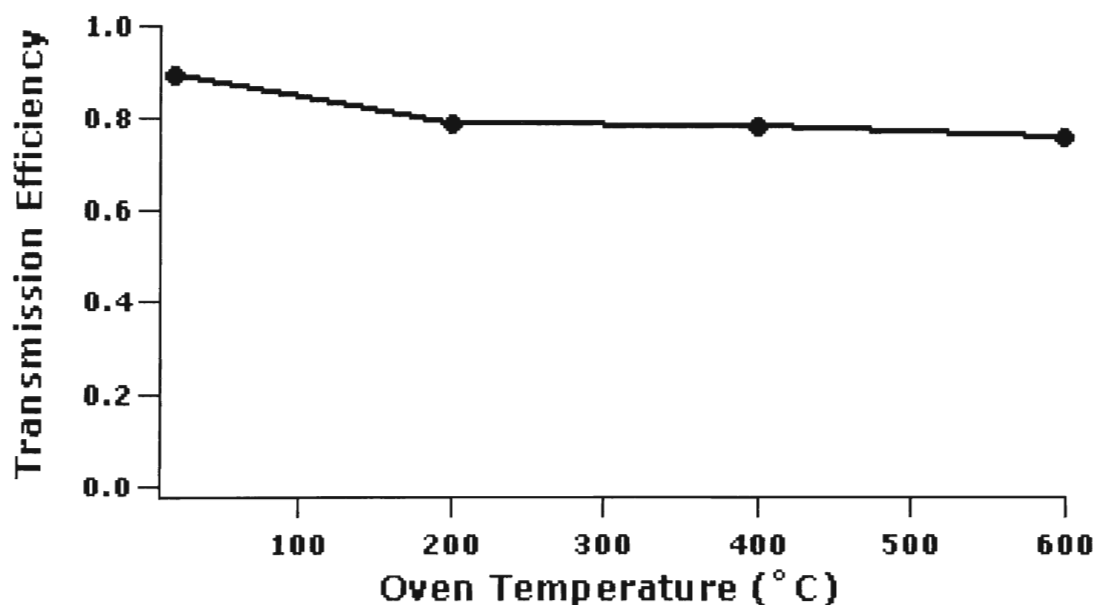
Figure 2. Transmission efficiency for aluminum.
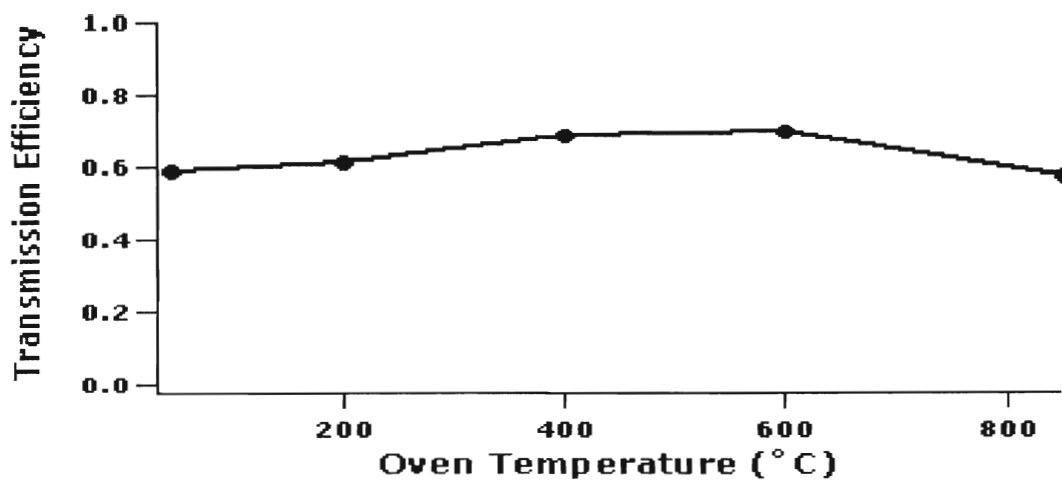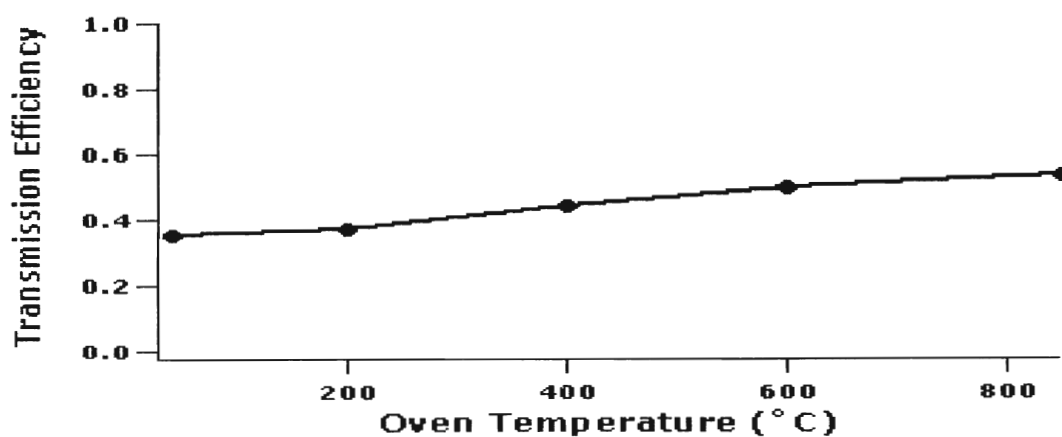
Figure 6. Transmission efficiency for palladium.

Figure 7. Transmission efficiency for platinum.
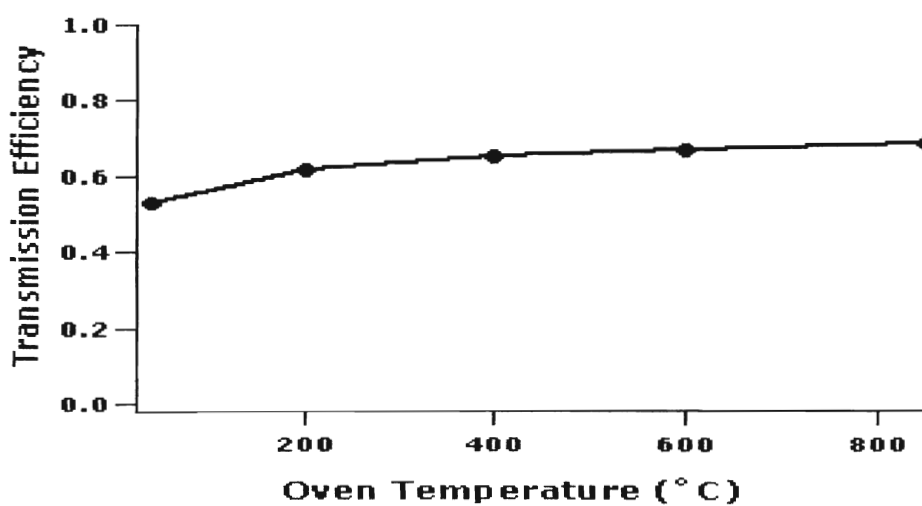
Figure 8. Transmission efficiency for silver.

24
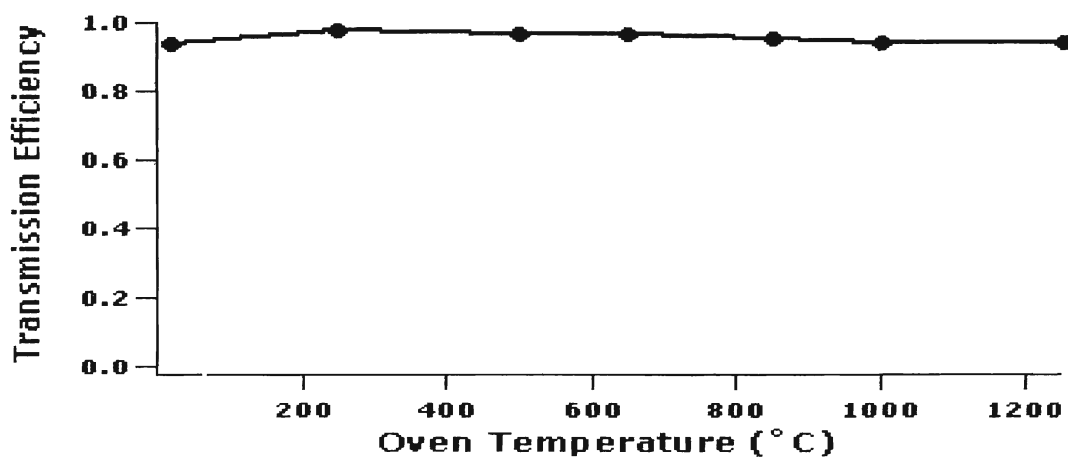
Figure 9. Transmission efficiency for stainless steel.
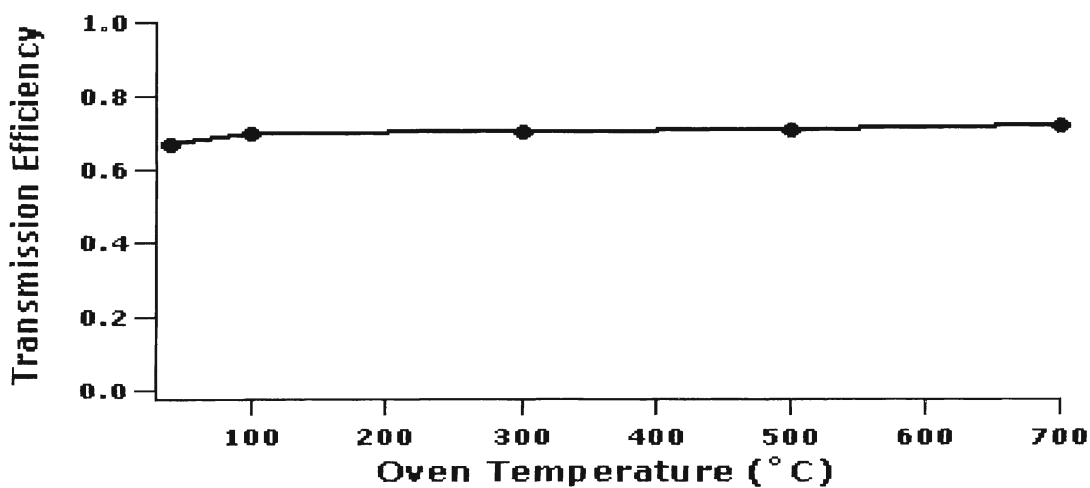
Figure 10. Transmission efficiency for vanadium.
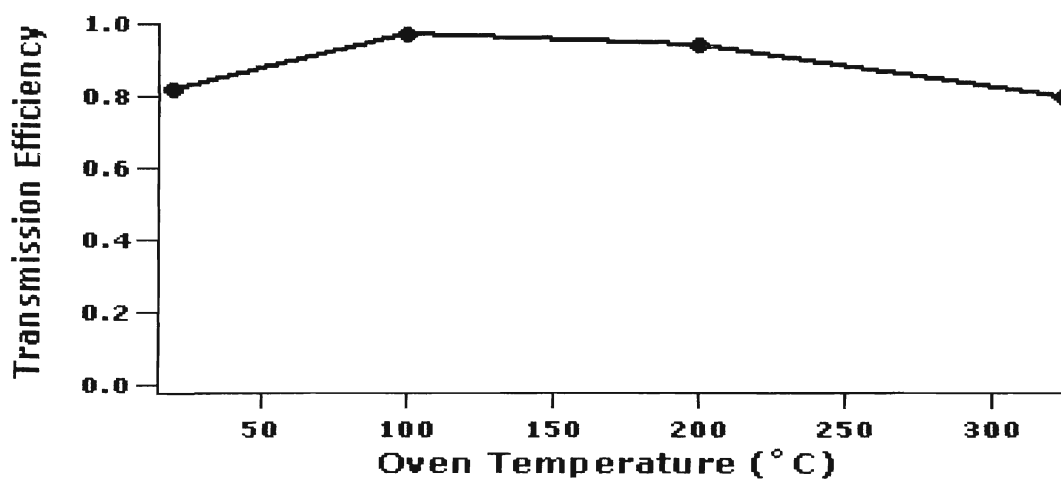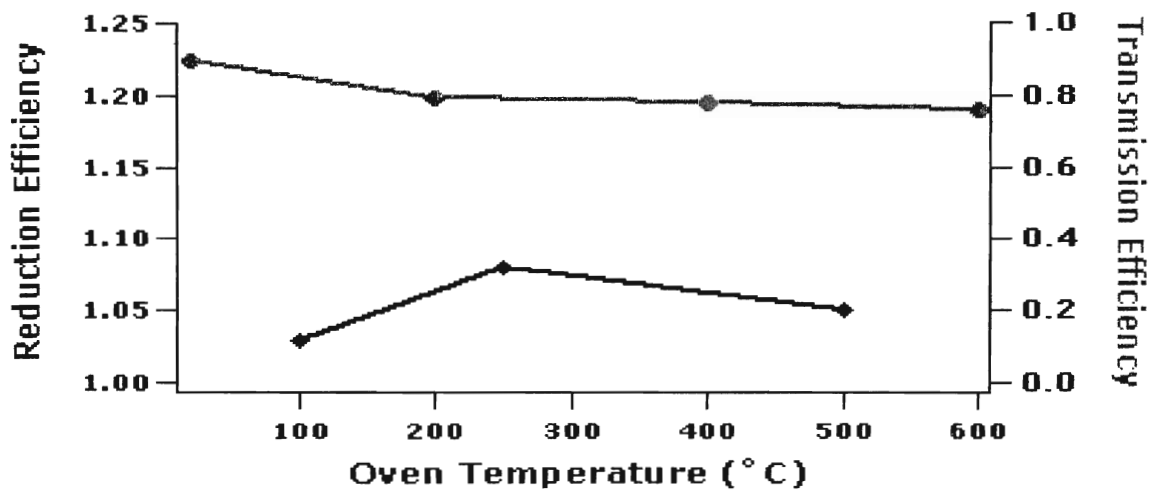

Figure 11. Transmission efficiency for zinc.

Figure 12. Reduction efficiency and transmission efficiency for aluminum.
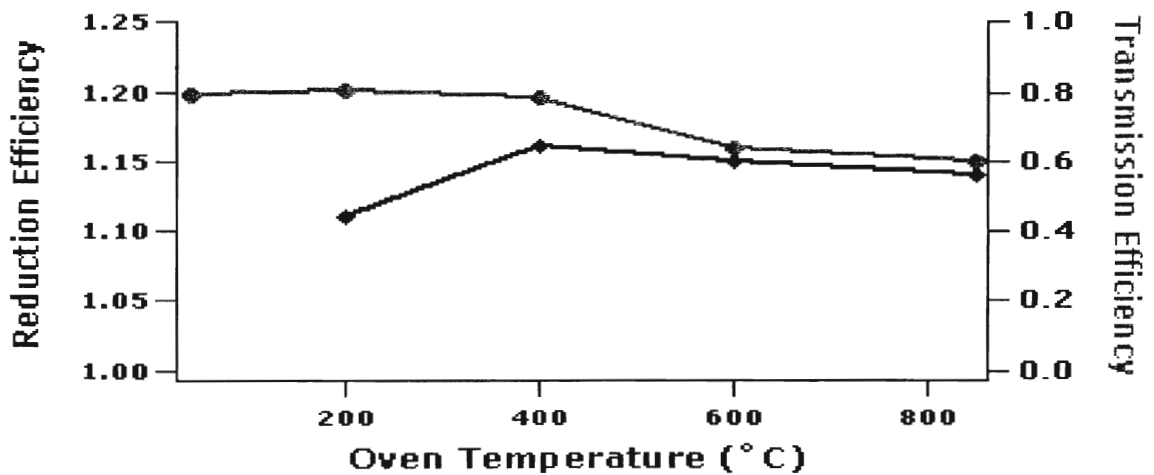

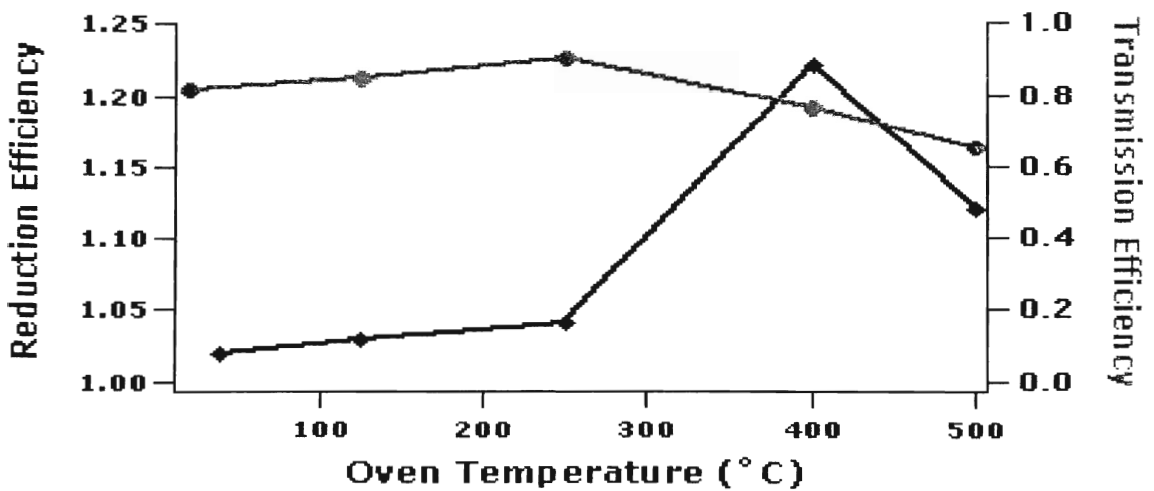Figure 13. Reduction efficiency and transmission efficiency for chromium.

Figure 14. Reduction efficiency and transmission efficiency for magnesium.
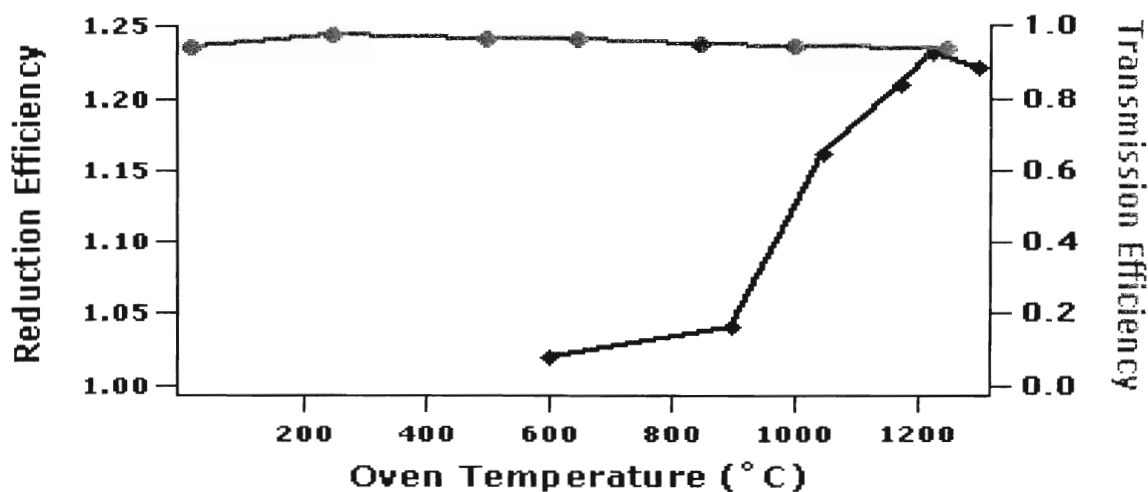
26

Figure 15. Reduction efficiency and transmission efficiency for stainless steel.
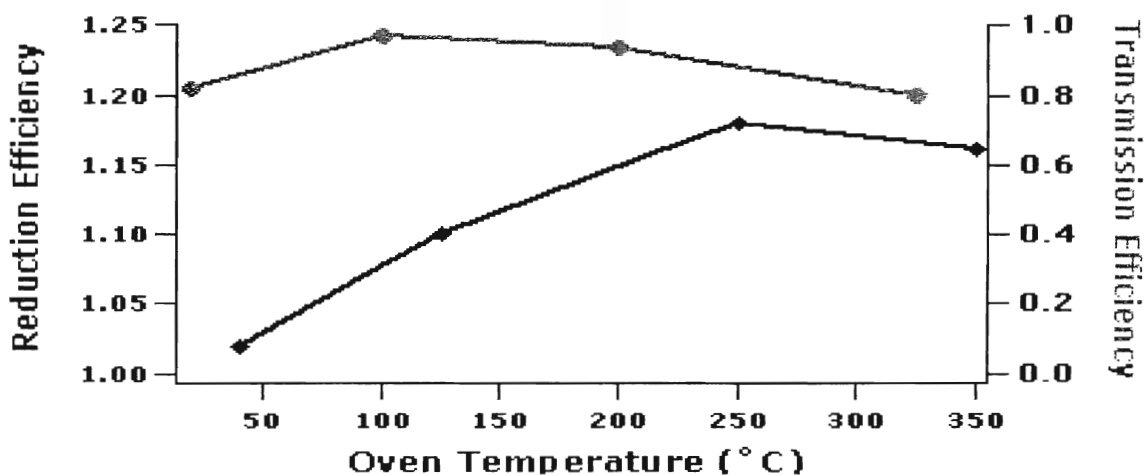

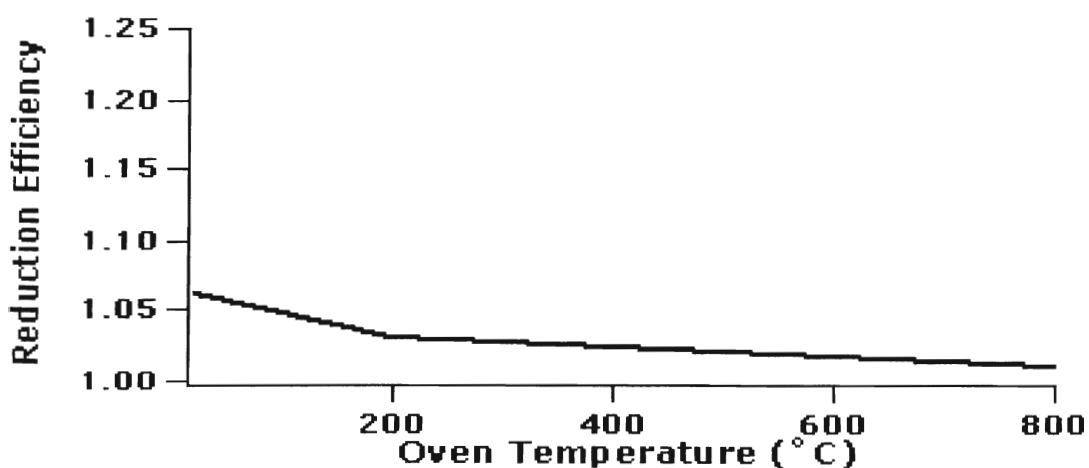Figure 16. Reduction efficiency and transmission efficiency for zinc.

Figure 17. Reduction efficiency for nickel.

Table 3 summarizes the maximum transmission efficiency and maximum reduction efficiency. A wide range of maximum transmission efficiencies was observed, from molybdenum's 0.475 to stainless steel's 0.976. This broad range of values may be explained by considering the radius of each metal. As the radius of the metal increases, the size of the octahedral or tetrahedral hole in the metal's crystal structure will also increase. Larger holes allow for more hydrogen to be absorbed by the metal, resulting in lower transmission efficiency. The effect of atomic radius on transmission efficiency is shown in Figure 18. A general trend shows the metals with smaller radii in the same row show greater transmission efficiencies.

A wide range in maximum reduction efficiencies was also observed, from 1.08 for aluminum to 1.23 for stainless steel. Figure 19 shows reduction efficiency as a function of standard reduction potential. There is a clearer trend that metals in the same period with more negative standard reduction potentials (easier to oxidize) show a greater reduction efficiency.

Only reduction efficiency was tested for nickel because this metal was obtained while the system was configured for these experiments. Because of the low reduction efficiency, it was not tested for transmission efficiency.

Table 3. Maximum transmission efficiency and reduction efficiency, standard reduction potential, and atomic radii.

Metal	Max. Trans. Eff.	Max. Red. Eff.	E° (in volts)[b]	Atomic Radii[a] (in Å)
Al	0.894	1.08	-1.662	1.43
Cr	0.800	1.17	-0.744	1.29
Mg	0.900	1.22	-2.372	1.60
Mo	0.475			1.40
Pd	0.695			1.37
Pt	0.537			1.39
Ag	0.681			1.44
Steel	0.976	1.23	-1.21[d]	1.26[c]
V	0.573			1.35
Zn	0.968	1.17	-0.7618	1.37
Ni		1.06	-0.257	

a. Shriver, D; Atkins, P, *Inorganic Chemistry*, 3rd edn. W. H. Freeman and Company, New York (1999)
b. CRC Handbook of Chemistry and Physics, 77th ed., 1996, given as most stable ion to metal.
c. Radius of iron
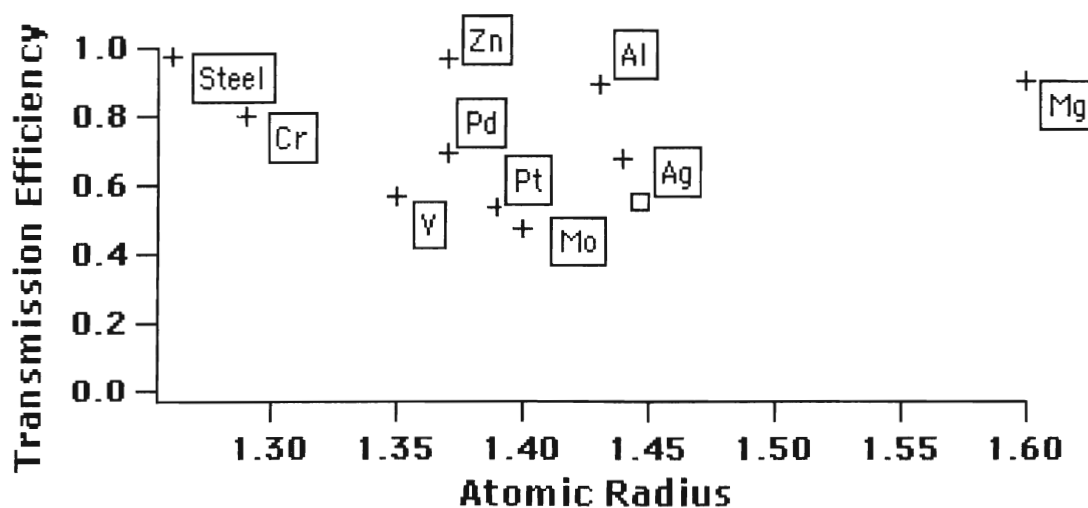d. E° of Fe^{3+} to Fe

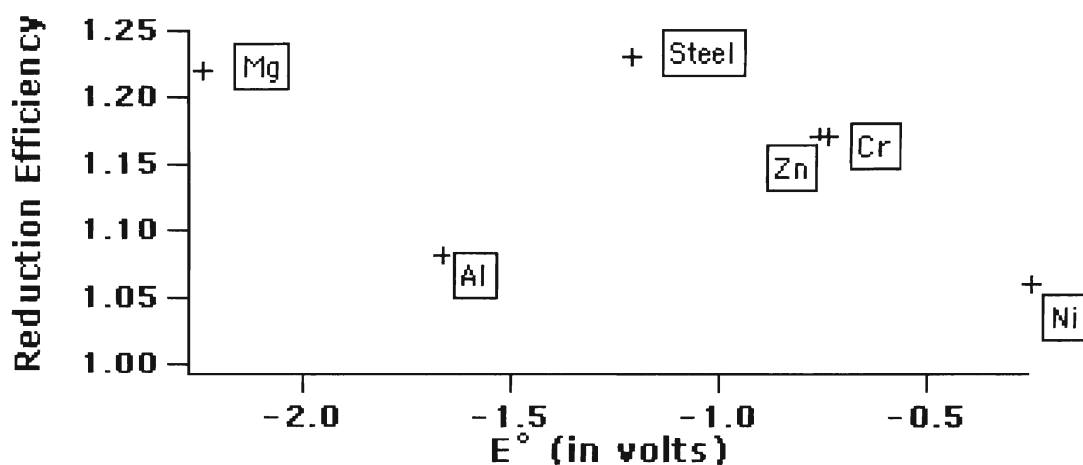Figure 18. Transmission efficiency as a function of atomic radius.

Figure 19. Reduction efficiency as a function of standard reduction potential in volts.

Stainless steel has the highest overall transmission efficiency, transmitting 97.6% of the hydrogen generated by pyrolysis. At the maximum reduction efficiency temperature, stainless steel transmits 96.5% of the hydrogen generated. It also has the highest reduction efficiency, reducing 98.4% of the HCl generated from pyrolysis. Therefore it was chosen as the best catalyst for the on-line reduction of HCl.

Further tests were conducted on stainless steel to optimize its performance. After repeating the reduction efficiency experiment three times using 12-inch alumina tubes, the experiment was repeated three additional times using 16-inch alumina tubes. By increasing the length, the number of catalytic sites was increased and the length of time the HCl spent in the reduction oven was also increased.

Figures 20 and 21 summarize the results for optimizing the

performance of stainless steel catalyst. A slight increase in maximum

reduction efficiency was observed at higher temperatures, while the

reduction efficiency at lower temperatures remained essentially

unchanged. With 12-inch alumina tubes, reduction efficiencies of 1.20

were consistently observed. This value correlates to 96.0% reduction

of HCl. Using 16-inch alumina tubes, reduction efficiencies of 1.23

were consistently observed. This value correlates to 98.4% reduction
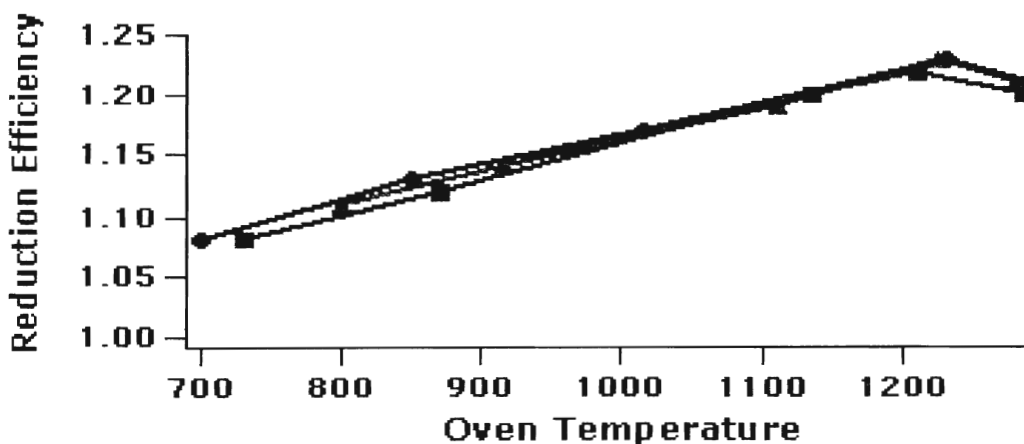
of HCl.

Figure 20. Reduction efficiency using 12-inch
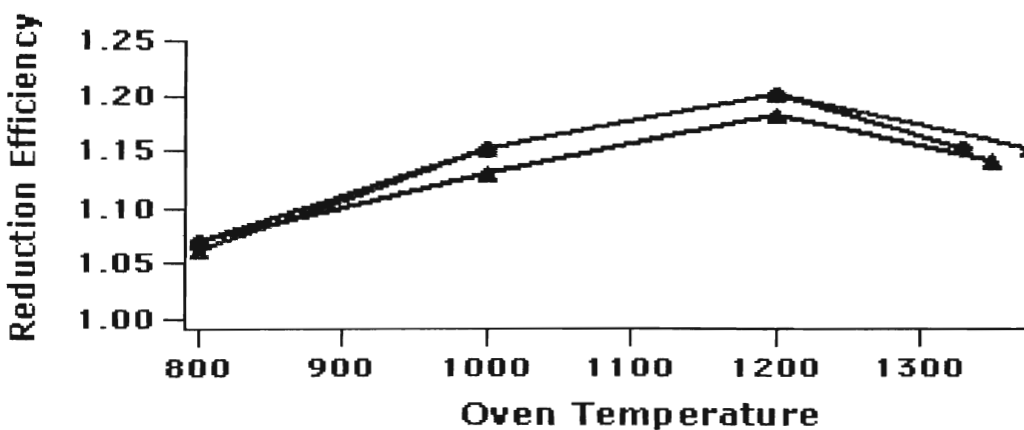alumina tubes.

Figure 21. Reduction efficiency using 16-inch
alumina tubes.

REDUCTION CAPACITY

Figure 22 shows the results for the reduction capacity test. Stainless steel effectively reduces ~2 x 10^{-8} moles of HCl before the reduction capacity begins to decrease.
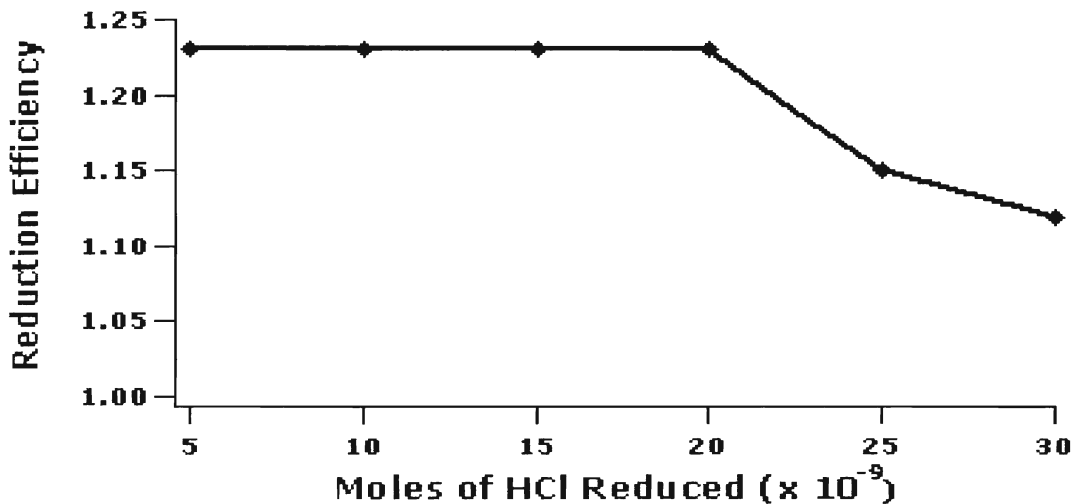

Figure 22. Reduction capacity of stainless steel.

EFFECTS OF LEAKS

Oxygen has serious effects on the reduction efficiency of stainless steel. Figures 23 and 24 are background scans before and after the simulated leak. A reduction efficiency of less than one (compared to 1.23 for a leak-free system) was observed; indicating some hydrogen had reacted and was no longer present as hydrogen gas, and therefore, no longer capable of detection. One possible hypothesis is water was produced in the reduction oven, as indicated by an increase in the peak at mass
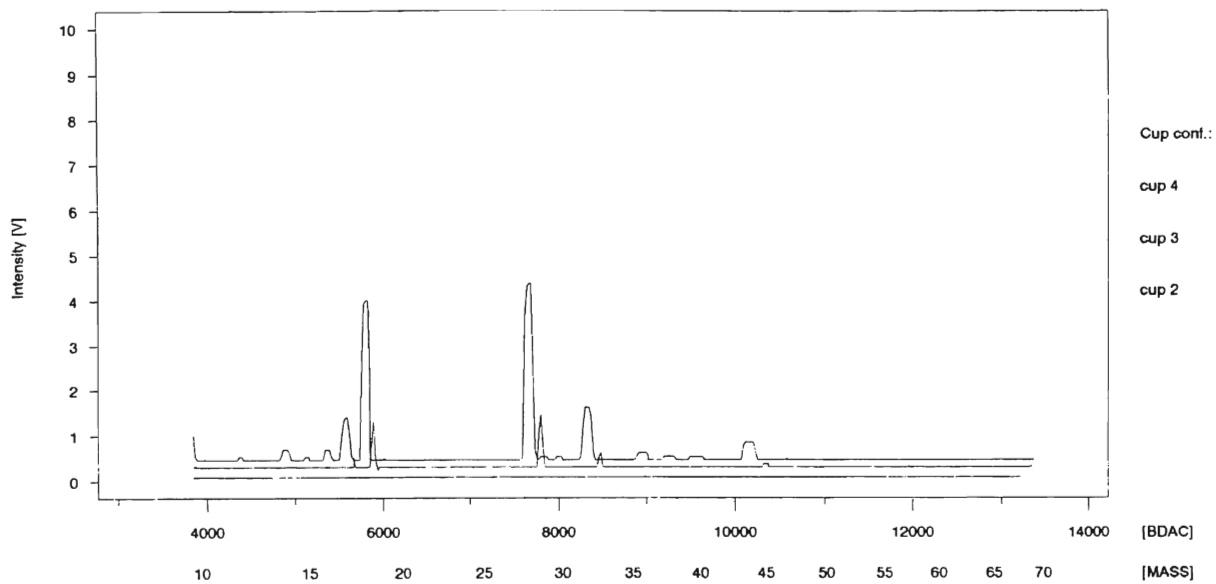
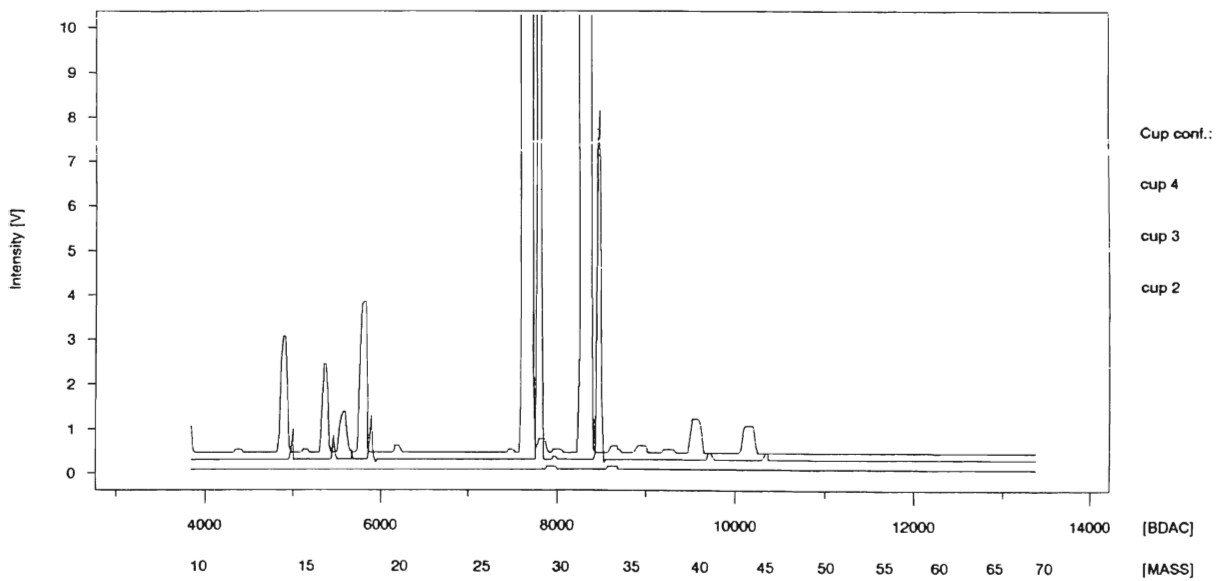Figure 23. Background scan before simulated leak.

Figure 24. Background scan after simulated leak.

18. Reduction efficiency decreased with time, possibly due to the formation of iron oxides and chromium oxides on the surface of the stainless steel.

Figure 25 show the reduction efficiency of stainless steel at various temperatures with a simulated leak, while Figure 26 shows reduction efficiency as a function of time. The results of these experiments indicate that the system must be kept leak free for the most accurate results.
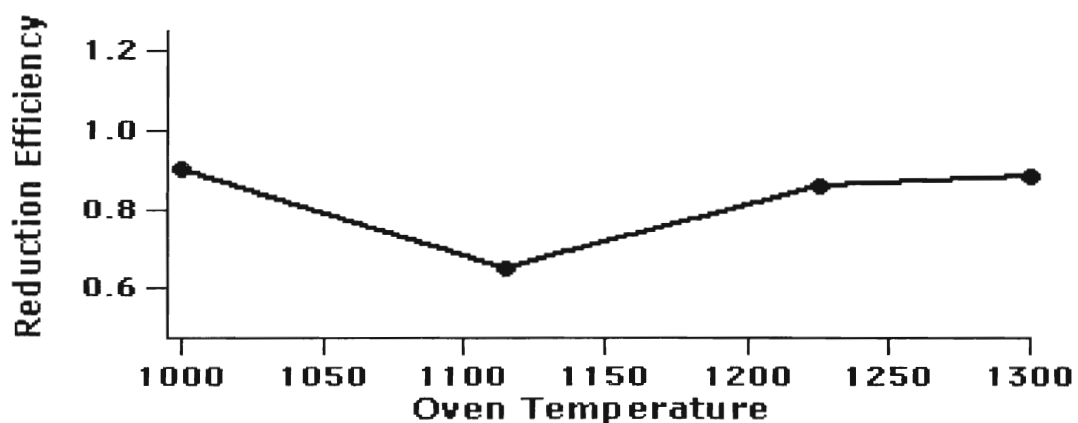

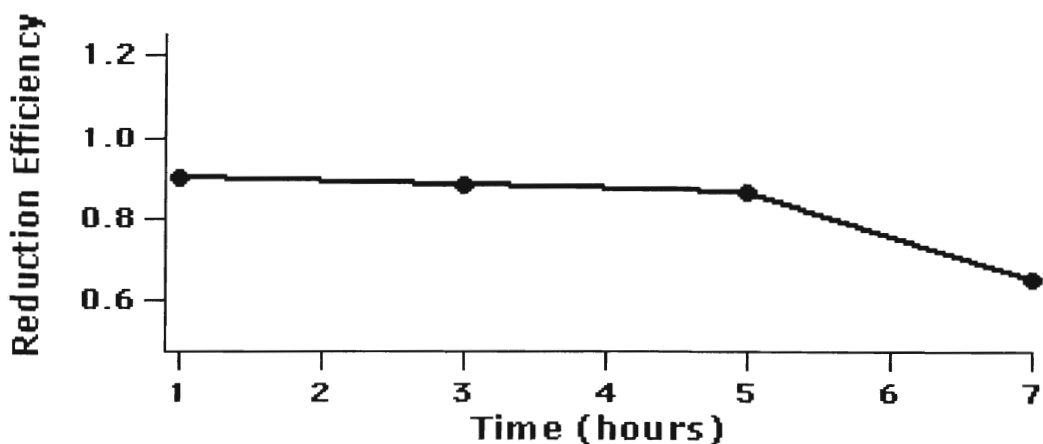Figure 25. Reduction efficiency at various temperatures in a simulated leak.

Figure 26. Reduction efficiency at various times during a simulated leak.

ON-LINE ANALYSIS OF PCBs

Table 4 summarizes the on-line δD values for the PCBs.

Table 4. On-line δD values (average and standard deviation)

PCB	Online δD (‰)	n	Offline δD (‰)	n
4-chloro	-52.0 ± 3.16	4	-52.8 ± 4.38	2
3,4-dichloro	-68.3 ± 1.91	5	-72.9 ± 5.91	2
2,3',4-trichloro	-72.6 ± 2.05	2	-25.0 ± 3.61	2
trichloro w/ dual reactor	-25.3 ± 4.08	4	-25.0 ± 3.61	2

The mono- and di- chlorobiphenyls are in excellent agreement with the off-line data, however the first attempt with the trichlorobiphenyl is significantly different from the off-line values.

The lack of accuracy for the trichlorobiphenyl is most likely due to an overload of HCl; simply too much HCl was produced for the system to effectively reduce. To test this, the reduction efficiency experiment was repeated twice at 1225 $^{\circ}$C using 1,2,3-trichloropropane (Aldrich Chemical, Milwaukee, WI) as the organochlorine molecule. Each injection contained approximately 10^{-9} moles of hydrogen and was injected via the GC. If all of the HCl was reduced, the reduction efficiency should be 2.5. However, these experiments gave an average reduction efficiency of 1.65, corresponding to only 66% reduction of the HCl generated, resulting in the significant deviation that was observed in the δD values.

In an attempt to correct for this saturation problem, a second

stainless steel-containing alumina tube was added in series to the reduction oven. Adding a second reactor effectively doubled the amount of time the HCl spent in the reactor, as well as effectively doubling the surface area of the catalyst. Adding this second reactor tube brought the trichlorobiphenyl δD values closer to the off-line values.

CONCLUSIONS

This project demonstrated it is now possible for on-line hydrogen-isotope analyses to be performed on hydrogen bound to atoms other than carbon and oxygen, in this study chlorine from PCBs. Using 302 stainless steel at 1225 $^{\circ}$C as a reducing catalyst for HCl, the number of compounds that may be analyzed quickly and easily has been expanded to include organochlorine molecules, many of which pose possible human health threats.

Stainless steel has high transmission efficiency, transmitting 96.5% of the hydrogen generated by pyrolysis of organic molecules at the maximum reduction efficiency temperature. It also has high reduction efficiency, reducing 98.4% of the hydrogen chloride generated by pyrolysis of organochlorine molecules.

With the current technology, peak widths are quite large,

36

approximately 2 minutes. With this system, only the simplest of chromatographic systems may be accurately analyzed. For complex environmental samples, this problem must be addressed. Figures 27 and 28 are representative chromatograms for hydrogen derived from 4-chlorobiphenyl and from 2,3',4-trichlorobiphenyl respectively.
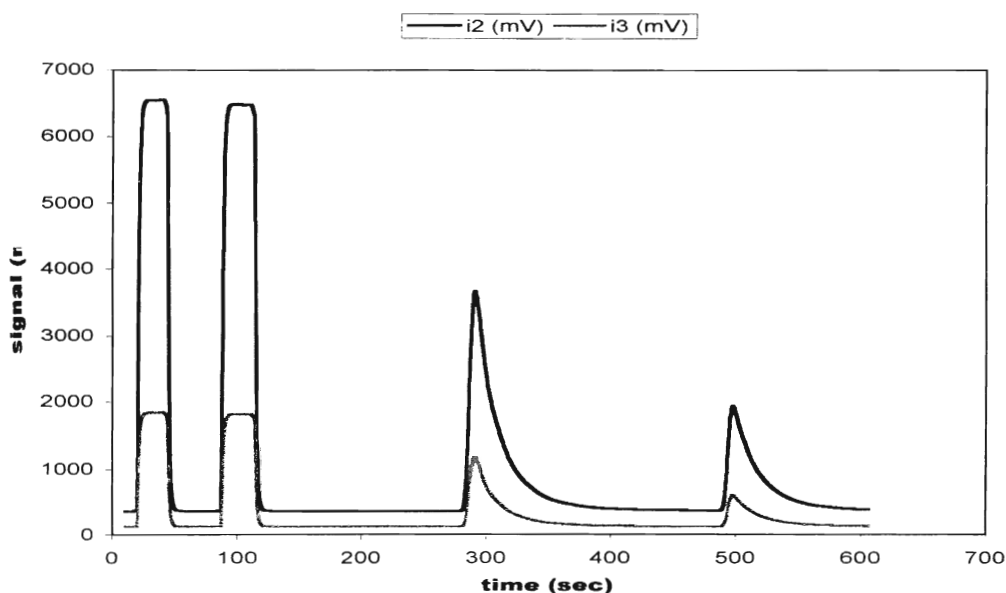

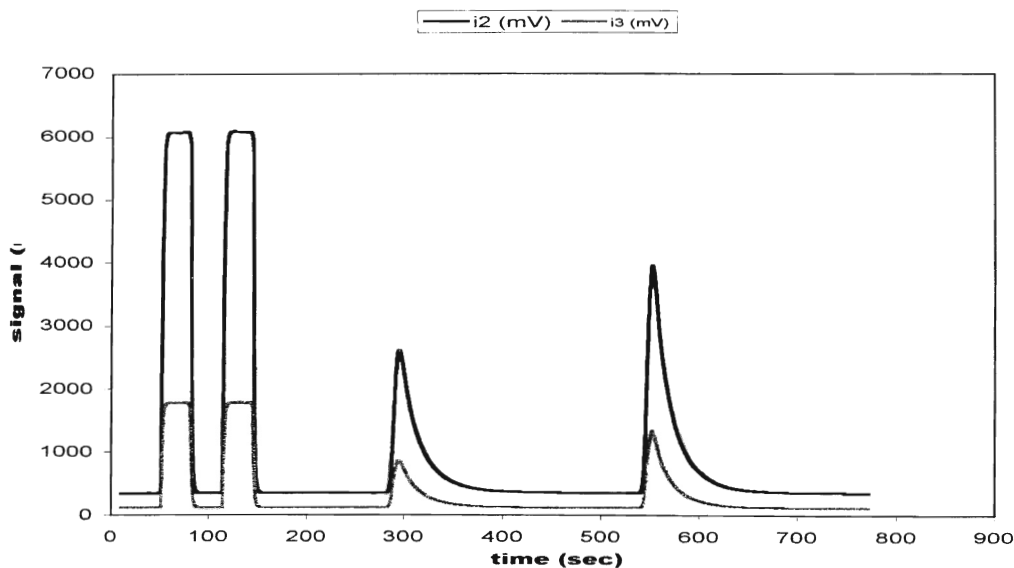Figure 27. Chromatogram for hydrogen derived from 4-chlorobiphenyl.

Figure 28. Chromatogram for hydrogen derived from 2,3',4-trichlorobiphenyl.

The stainless steel reactor must be changed frequently, as it has

a somewhat low reduction capacity, resulting from its relatively small surface area. Using a powder, a gauze, or a honey-comb type structure may increase the reduction capacity, by greatly increasing the surface area. However, these may disrupt the laminar flow of the gases causing further band broadening. Another possible solution may be to completely remove HCl from the system and enter a correction factor in the same manner as an H_3^+ factor. Another option may be to reduce the iron ions and chromium ions back to iron metal and chromium metal.

Despite these drawbacks, this system is a significant improvement over past methods of analysis.

REFERENCES

1. Schimmelmann, A; Lewan, M. D.; Wintsch, R. P. *Geochim. Com. Acta* **1999**, 63, 3751

2. Smallwood, ,B. J. *et al. Environ. Foren.* **2001**, 2, 215

3. Li, M.; *et al. Organic Geochem.* **2001**, 32, 1387

4. Ruff, C.; *et al. Journal High Res. Chrom.* **2000**, 23, 357

5. Sessions, A. L.; *et al. Organic Geochem.* **1999**, 30, 1193

6. Ward, J. E.; *et al. Environ. Sci. Tech.* **2000**, 34, 4577

7. Pond, K. L.; *et al. Environ. Sci. Tech.* **2002**, *36*, 724

8. Nier, A. O. *Rev. Sci. Inst.* **1940**, 11, 212

9. de Hoffman, E; Stroobant, V *Mass Spectrometry Principles and Applications Second ed.;* Wiley and Sons, LTD, Chichester, 2001

10. Nier, A. O.; *Rev. Sci. Inst.* **1947**, 18, 398

11. McKinney, C. R.; et al *Rev. Sci. Inst.* **1950**, 21, 724

12. Hachey, D. L. et al, *Mass Spec. Rev.* **1987**, 6, 289

13. Wong, W. W.; Klein. P. D. *Rev. Mass Spec.* **1986**, 5, 313

14. Brenna, J. T. *Acc. Chem. Res.* **1994**, 27, 340

15. Sano, M.; et al *Biomed. Mass Spec.* **1976**, 3, 1

16. Matthews, D. E.; Hayes, J. M. *Anal. Chem.* **1978**, 50, 1465

17. Brenna, J. T.; et al *Mass Spec. Rev.* **1997**, 16, 227

18. Tobias, H. J.; et al *Anal. Chem.* **1995**, 67, 2486

19. Hoefs, J.; *Stable Isotope Geochemistry Fourth ed.*; Springer Press, Berlin, 1997

20. Burgoyne, T. W. Hayes, J. M.; *Anal. Chem.* **1998**, 70, 5136

21. Midwood, A. J.; McGraw, B. A. *Anal. Comm.* **1999**, 36, 291

22. Begley, I.S.; Scrimgeour, C. M. *Anal. Chem.* **1997**, 69, 1530

23. Merren, T. *Micromass Technical Brief,* **2000,** TB4

24. Hilkert, A. W. et al; *Rapid Comm. Mass Spec.* **1999**, 13, 1226

25. Sessions, A. L.; Burgoyne, T. W.; Hayes, J. M. *Anal. Chem.* **2001**, 73, 192

26. Sessions, A. L.; Burgoyne, T. W.; Hayes, J. M. *Anal. Chem.* **2001**, 73, 200.

27. Tavakoli, J.; Doney, J. A. *Chem. End Comm.* **1993**, 119, 135

28. Tavakoli, J.; Chiang, H. M.; Bozzelli, J. W. *Combust. Sci. Technol.* **1994**, 101(1-6), 135

29. Taylor, P. H.; et al *Combust. Sci. Technol.* **1994**, 101(1-6), 75

30. Taylor, P. H.; Tirey, D. A.; Dellinger, B. *Combust. Flame* **1996**, 104, 260

31. Won, Y. S.; Bozzelli, J. W. *Combust. Sci. Tech.* **1992**, 85(1-6), 345

32. Schimmelman, A; Personal Communication, 2002

VITA 2

William Rhea Alley, Jr.

Candidate for the degree of

Masters of Science

Thesis: DEVELOPMENT OF HYDROGEN ISOTOPE-RATIO MASS
SPECTROMETRY FOR ORGANOCHLORINE MOLECULES

Major Field: Chemistry

Education: Received Bachelor of Science Degrees in Chemistry and
Chemistry Education from Dickinson State University, Dickinson,
North Dakota in May, 2000. Completed requirements for the
degree of Masters of Science from Oklahoma State University,
Stillwater, Oklahoma in August, 2002.

Experience: Teaching Assistant, 2001-2002.